Potts Model with Competing Interaction Up to the Third Nearest-neighbour Generation on a Cayley Tree

Nasir Ganikhodjaev[a], Mohd Hirzie Mohd Rodzhan[a] and Sahira Basirudin[a]

[a]Department of Computational and Theoretical Sciences, International Islamic University Malaysia Kuantan, Jalan Sultan Ahmad Shah, 25200 Kuantan, Pahang, Malaysia.

(Received: 13.6.2019 ; Published: 3.12.2019)

Abstract. It is in our interest to investigate the effect of the third nearest-neighbour binary interaction to the phase diagrams of the Potts model on a Cayley tree. Therefore, we generate and analyse the phase diagrams of the Potts model, considering prolonged competing binary interaction J_2 and J_3 on the same branch of the Cayley tree up to the third nearest-neighbour generations. We derive the recurrence system of equations while taking into account some ranges of competing parameters. We carry out a numerical procedure by applying several stability conditions and characteristic points into the iteration scheme. For some non-zero parameter J_3, we found the additional phases of period 5, 6, 9, and 11, with the ferromagnetic, antiphase, paramagnetic, antiferromagnetic and modulated phase. For the modulated phase, we further study the existence of phases with period larger than 12 by conducting a numerical analysis on the variation of wavevector and Lyapunov exponent.

Keywords: Cayley tree, competing interaction, phase diagram, Potts model, statistical mechanics.

I. INTRODUCTION

Statistical mechanics is one of the fundamental aspects of modern physics. It aims to predict the relations between the observable macroscopic properties of the system, given only a knowledge of the microscopic forces between the components, as has been mentioned by Baxter [1]. This enables us to investigate some thermodynamic properties by having the knowledge of the interactions between the lower level entities. Among many models being studied in statistical mechanics, one of them is the Potts model. It was introduced by Renfrey Potts [2] in his 1952 doctoral thesis. Today, the model is widely known as the *q*-state Potts model. Potts model is actually the generalisation of the Ising model, extending the model to more than two interacting spins on a lattice. In this paper, we are particularly intrigued in studying the phase transition of a lattice gas model. This is accomplished by studying its phase diagram, which illustrates the stability and morphology of phases, transition from a phase to another and the corresponding transitions line.

This paper will follow closely the methodology that was introduced by Vannimenus [3]. He had studied the phase diagram of the Ising model with competing and prolonged second nearest-neighbour interactions on the Cayley tree and successfully found a new modulated phase. His work was further developed by Inawashiro [4], where in this paper; a chaotic oscillatory glass represents the local magnetization of the model.

Further to the previous research, Mariz, Tsallis and Albuquerque [5] had investigated the phase diagrams of the Ising model with the first and second nearest-neighbour interaction for one-level and prolonged with the presence of external magnetic field. They found that, at low temperature, there are more than one critical point. Moreover, Ganikhodjaev and Mohd Rodzhan [6] studied the phase diagram of the Ising model on the Cayley tree with competing interactions up to the third nearest-neighbour, which considers spins belonging to the different branches of the tree. It is defined as the 'Uncle-Nephew' interactions by Ganikhodjaev [7]. In addition to the expected ferromagnetic, anti-ferromagnetic and paramagnetic phases, they have shown the existence of a new paramodulated phase in the phase diagram.

Not only that, they also examined the phase diagram of the Ising model on Cayley tree with competing first, second, and third nearest-neighbor interactions in the following year by Ganikhodjaev and Mohd Rodzhan [8]. It has been found in this paper that the third nearest-neighbor interactions are crucial for the existence of a periodic < + + + - - - > antiphase <3>.

In investigating the Potts model, previously, Ganikhodjaev, Mukhamedov and Pah [9] had considered the Potts model with competing and second nearest-neighbour interactions on the Cayley tree, which further generalized the result of [2]. Consequently, they have shown the paramodulated phase, which is determined by zero average magnetization and came into existence in low temperature. Other than that, Ganikhodjaev, Temir and Akin [10] investigated the phase diagram for Potts model on the Cayley tree with competing prolonged and one-level second nearest-neighbour interactions. In this paper, the paramagnetic phase found at high temperatures for $J_0 = 0$ has been proven to disappear as the same-level interaction J_0 becomes nonzero. More models that are considered on the Cayley tree can be further read in Rozikov [11].

This paper aims to further develop the results of Ganikhodjaev, Mukhamedov and Pah [9] to the Potts model on the Cayley tree with competing first, prolonged second and third nearest-neighbour. The main result is that there is a substantial effect on the phase diagram as we consider the binary interaction on the Cayley tree up to the third nearest-neighbour. For some non-zero parameter J_3, we found the additional phases of period 5, 6, 9, and 11, as well as the ferromagnetic, antiphase, paramagnetic, antiferromagnetic and modulated phase.

II. THE MODEL HAMILTONIAN

In this section, we will provide some definitions for the terms that will be crucial throughout our study. A Cayley tree Γ^k of order $k \geq 1$ is an infinite tree, which is a graph without cycles with exactly $k + 1$ edges issuing from each vertex. We denote the Cayley tree as $\Gamma^k=(V, \Lambda)$, where V is the set of vertices on Γ^k and Λ is the set of edges on Γ^k. Two vertices x and y, $x, y \in V$ are called the *first nearest-neighbour*, if there is an edge $l \in \Lambda$ connecting them, denoted by $l = <x, y>$.The distance $d(x, y)$, $x, y \in V$ on the Cayley tree is the number of edges which make the shortest path from x to y. For a fixed set $x^0 \in V$, we set

$$W_n = \{x \in V \mid d(x, x^0) = n\}, V_n=\{x \in V \mid d(x, x^0) \leq n\}$$

and L_n denotes the set of edges in V_n. The fixed vertex x^0 is called the 0-th level and the vertices x in W_n are called the n-th level. Further, we put $|x| = d(x, x^0)$, $x \in V$.

Two vertices $x, y \in V$ are called the *second nearest-neighbours* if $d(x, y) = 2$. They are called *prolonged second nearest-neighbors* if $|x| \neq |y|$ and are denoted by $>\widetilde{x, y}<$. On the other hand, the vertices $x, y \in V$ are called the *third nearest-neighbor* if $d(x, y) = 2$. They are called *prolonged*

third nearest-neighbours if $x \in W_n$, $y \in W_{n+3}$ for some n and is denoted by $\widetilde{<x, y>}$.The notation $x \prec y$ is used if the path from x^0 to y goes through x. The vertex y is called a *direct successor* of x, if $y \succ x$ and x, y are nearest-neighbors. The set of the direct successors of x is denoted by $S(x)$, hence if $x \in W_n$, then

$$S(x) = \{y_i \in W_{n+1} \mid d(x, y_i) = 1,\ i=1, \ldots, k\}.$$

Throughout the study, we consider a semi-infinite Cayley tree Γ_+^2 of order 2 that is an infinite graph without cycles with three edges branching out from each vertex except for x^0, which consists of only two edges. We are investigating on a three-state Potts model with spin values $\phi = \{1, 2, 3\}$. Therefore, the relevant Hamiltonian with competing first, second and third nearest-neighbour binary interaction has the form

$$H(\sigma) = -J_1 \sum_{<x, y>} \delta_{\sigma(x)\sigma(y)} - J_2 \sum_{>\widetilde{x,y}<} \delta_{\sigma(x)\sigma(y)} - J_3 \sum_{<\widetilde{x,y}>} \delta_{\sigma(x)\sigma(y)} \tag{1}$$

where first term includes all *first nearest-neighbors*, the second one comprises all *prolonged second nearest-neighbors' interactions* and the third sum consists of all *prolonged third nearest-neighbors*. Moreover, the spin variables $\sigma(x)$ assume the values 1, 2, and 3. Furthermore, J_1, J_2, $J_3 \in \mathbb{R}$ are coupling constants while δ is defined as the Kronecker symbol, i.e.

$$\delta_{\sigma(x)\sigma(y)} = \begin{cases} 1 & \text{if } \sigma(x) = \sigma(y) \\ 0 & \text{if } \sigma(x) \neq \sigma(y) \end{cases}$$

For the purpose of this study, we are we are taking into account all values of J_1 and J_2, as well as some non-zero J_3.

III. BASIC EQUATIONS

First and foremost, we derive the recurrence system of equations as introduced by Vannimenus [2]. We consider the relation of the partition functions on V_n into the subsets of V_{n-1}. Let us denote $V_2 = (x^0, y^1, y^2, z^1, z^2, z^3, z^4)$, where $S(x^0) = (y^1, y^2)$, $S(y^1) = (z^1, z^2)$ and $S(y^2) = (z^3, z^4)$.

The recurrence equations demonstrate the transmission of their influence throughout the tree, provided that the initial condition for V_2 is given. Let

$$\sigma(V_2) = \begin{pmatrix} \sigma(z^1), \sigma(z^2), \sigma(z^3), \sigma(z^4) \\ \sigma(y^1), \sigma(y^2) \\ \sigma(x^0) \end{pmatrix} \tag{2}$$

set of all configurations on V_2. We assume

$$a = \exp(\beta J_1),\ b = \exp(\beta J_2) \text{ and } c = \exp(\beta J_3), \tag{3}$$

where β is the inverse temperature, then

$$\begin{aligned} Z^n(\sigma(V_2)) = a^{\delta_{\sigma(x^0)\sigma(y^2)} + \delta_{\sigma(x^0)\sigma(y^1)}} . b^{\delta_{\sigma(x^0)\sigma(z^1)} + \delta_{\sigma(x^0)\sigma(z^2)} + \delta_{\sigma(x^0)\sigma(z^3)} + \delta_{\sigma(x^0)\sigma(z^4)}} \\ \cdot Z^n(\sigma(x^0), \sigma(y^1), \sigma(z^1)) \cdot Z^n(\sigma(x^0), \sigma(y^1), \sigma(z^2)) \\ \cdot Z^n(\sigma(x^0), \sigma(y^1), \sigma(z^3)) \cdot Z^n(\sigma(x^0), \sigma(y^1), \sigma(z^4)) \cdot \end{aligned} \tag{4}$$

be the partition function on V_n with fixed $\sigma(V_2)$. Hence, there are 2187 partitions functions $Z^n(\sigma(V_2))$. Next, we can show that there exist 14 independent variables of $Z^n(\sigma(V_2))$.The partition function Z^n in volume V_n is denoted as $Z^n = \sum_{\sigma(V_2)\in\Omega(V_2)} Z^n(\sigma(V_2))$. The variables are defined as follows

$$u_1=\sqrt[4]{Z^n\begin{pmatrix}1,1,1,1\\1,1\\1\end{pmatrix}},\quad u_2=\sqrt[4]{Z^n\begin{pmatrix}2,2,2,2\\1,1\\1\end{pmatrix}},\quad u_3=\sqrt[4]{Z^n\begin{pmatrix}1,1,1,1\\2,2\\1\end{pmatrix}},$$

$$u_4=\sqrt[4]{Z^n\begin{pmatrix}3,3,3,3\\3,3\\1\end{pmatrix}},\quad u_5=\sqrt[4]{Z^n\begin{pmatrix}2,2,2,2\\3,3\\1\end{pmatrix}},\quad u_6=\sqrt[4]{Z^n\begin{pmatrix}1,1,1,1\\1,1\\2\end{pmatrix}},$$

$$u_7=\sqrt[4]{Z^n\begin{pmatrix}3,3,3,3\\1,1\\3\end{pmatrix}},\quad u_8=\sqrt[4]{Z^n\begin{pmatrix}3,3,3,3\\1,1\\2\end{pmatrix}},\quad u_9=\sqrt[4]{Z^n\begin{pmatrix}1,1,1,1\\3,3\\3\end{pmatrix}},\qquad (5)$$

$$u_{10}=\sqrt[4]{Z^n\begin{pmatrix}2,2,2,2\\2,2\\2\end{pmatrix}},\quad u_{11}=\sqrt[4]{Z^n\begin{pmatrix}2,2,2,2\\3,3\\3\end{pmatrix}},\quad u_{12}=\sqrt[4]{Z^n\begin{pmatrix}1,1,1,1\\3,3\\2\end{pmatrix}},$$

$$u_{13}=\sqrt[4]{Z^n\begin{pmatrix}3,3,3,3\\2,2\\3\end{pmatrix}},\quad u_{14}=\sqrt[4]{Z^n\begin{pmatrix}3,3,3,3\\3,3\\2\end{pmatrix}},$$

Next, we establish the recursive relations as follows

$$u_1' = \sqrt{a}b(cu_1+2u_2)^2,\quad u_2' = \sqrt{a}(cu_3+u_4+u_5)^2,\quad u_3' = b(cu_6+u_7+u_8)^2,$$

$$u_4' = (cu_9+u_{10}+u_{11})^2,\quad u_5' = (cu_{12}+u_{14}+u_{13})^2,\quad u_6' = (cu_2+u_1+u_2)^2,$$

$$u_7' = b(cu_4+u_3+u_5)^2,\quad u_8' = (cu_5+u_3+u_4)^2,\quad u_9' = \sqrt{a}(cu_7+u_6+u_8)^2,\qquad (6)$$

$$u_{10}' = \sqrt{a}b(cu_{10}+u_9+u_{11})^2,\quad u_{11}' = \sqrt{a}(cu_{13}+u_{12}+u_{14})^2,\quad u_{12}' = (cu_8+u_6+u_7)^2,$$

$$u_{13}' = b(cu_{14}+u_{12}+u_{14})^2,\quad u_{14}' = (cu_{11}+u_9+u_{10})^2,$$

where the above variables u_i' correspond to $u_i^{(n+1)}$. In the high symmetry (paramagnetic) phase, we consequently have $u_1 = u_{10}$, $u_2 = u_9 = u_{11}$, $u_3 = u_7 = u_{13}$, $u_4 = u_6 = u_{14}$, $u_5 = u_8 = u_{12}$. For the purpose of discussing the phase diagram, it is best to know that we have reduced the variables as follows

$$x_1=\frac{2u_2+u_9+u_{11}}{u_1+u_{10}},\quad x_2=\frac{2u_3+u_7+u_{13}}{u_1+u_{10}},$$

$$x_3=\frac{2u_4+u_6+u_{12}}{u_1+u_{10}},\quad x_4=\frac{2u_5+u_8+u_{12}}{u_1+u_{10}},$$
$$y_1=\frac{u_1-u_{10}}{u_1+u_{10}},\quad y_2=\frac{u_2-u_9}{u_1+u_{10}},\quad y_3=\frac{u_2-u_{11}}{u_1+u_{10}},$$
$$y_4=\frac{u_3-u_7}{u_1+u_{10}},\quad y_5=\frac{u_3-u_{13}}{u_1+u_{10}},\quad y_6=\frac{u_4-u_6}{u_1+u_{10}},$$
$$y_7=\frac{u_4-u_{14}}{u_1+u_{10}},\quad y_8=\frac{u_5-u_8}{u_1+u_{10}},\quad y_9=\frac{u_5-u_{12}}{u_1+u_{10}},$$

(7)

Hence, we obtain the following recurrence system of equations

$$x_1^{(n+1)}=\frac{1}{2bD}(6cy_4y_6-2cy_4y_7+6cy_5y_7+6y_6y_8-2y_7y_8-2cy_5y_6+x_4^2+3y_8^2+3y_9^2-2y_6y_9+x_3^2$$
$$+3y_7^2+3y_6^2+6cy_4y_8-2cy_4y_9+6cy_5y_9-2y_8y_9+2x_3x_4+6y_7y_9+c^2x_2^2-2y_6y_7-2c^2y_4y_5$$
$$+3c^2y_5^2+2cx_2x_4-2cy_5y_8+2cx_2x_3+3c^2y_4^2)$$

$$x_2^{(n+1)}=\frac{1}{2\sqrt{a}D}(-2x_4y_8-4y_4y_5-4y_5y_8-2x_2y_4-2y_4x_4-2x_2y_8+3c^2y_7^2+5c^2y_6^2-2cy_6x_2+10cy_4y_6$$
$$-4c^2y_6y_7-2c^2x_3y_6-4cy_4y_7+6cy_5y_7-4cy_6y_9+6cy_7y_9-2cx_3y_4-2cy_6x_4-4cy_7y_8$$
$$-4cy_5y_6+x_2^2+x_4^2+5y_4^2+3y_5^2+5y_8^2+3y_9^2-4y_8y_9+6y_5y_9+2x_2x_4+c^2x_3^2+10y_4y_8$$
$$-4y_4y_9+2cx_3x_4+2cx_2x_3-2cx_3y_8+10cy_6y_8)$$

$$x_3^{(n+1)}=\frac{1}{2\sqrt{a}bD}(4-4y_1+2cy_1y_3+6cy_1y_2-2cy_1x_1+4x_1+5y_3^2-4y_2y_3+3y_2^2+4cx_1-4cy_2$$
$$+16cy_2y_3-2c^2x_1y_2-2cx_1y_2-2cx_1y_3-4c^2y_2y_3+c^2x_1^2+2cx_1^2+5c^2y_2^2-4cy_2^2+3c^2y_3^2$$
$$-4y_3-4cy_3^2-2x_1y_1+2y_2y_1+6y_3y_1+4y_1^2+x_1^2-2x_1y_3)$$

$$x_4^{(n+1)}=\frac{1}{2\sqrt{a}bD}(6cy_6y_8+5y_7^2+3y_6^2-4y_4y_5-2x_3y_5+x_2^2+x_3^2+c^2x_4^2+3c^2y_8^2+5c^2y_9^2-2x_3y_7$$
$$+2x_3x_2-2x_2y_5-2y_7x_2-4y_7y_4+10y_7y_5-4y_6y_7-4cy_5y_8+10cy_7y_9-4cy_6y_9+10cy_5y_9$$
$$+2cx_2x_4+2cx_3x_4+6cy_4y_8-2c^2x_4y_9-2cy_9x_2-4cy_7y_8-2cx_4y_5-2cx_4y_7-4c^2y_8y_9-4cy_4y_9$$
$$-4y_6y_5+6y_6y_4-2cy_9x_3+5y_5^2+3y_4^2)$$

$$y_1^{(n+1)}=\frac{2}{D}(c^2y_1+cy_2+cy_3+x_1y_3+x_1y_2+cy_1x_1)$$

$$y_2^{(n+1)}=\frac{1}{bD}(cy_4y_7+c^2x_2y_4+cx_2y_8+cx_3y_4+cy_4x_4+cy_4y_9-2cy_4y_8+cy_5y_6+cy_5y_8+c^2y_4y_5$$
$$+y_7y_8+x_4y_8-2y_6y_8-2cy_4y_6+cy_6x_2+y_6x_4+x_3y_8-c^2y_4^2+y_6y_7+x_3y_6-y_8^2+y_6+y_8y_9-y_6^2)$$

$$y_3^{(n+1)}=\frac{1}{bD}(-y_9^2-y_7^2+y_7y_8+x_4y_9+x_3y_9-2y_7y_9+y_8y_9+y_6y_9+cy_9x_2+cy_5y_8+c^2y_4y_5+cy_4y_7$$
$$-2cy_5y_7+cy_5y_6+cy_4y_9-2cy_5y_9+cy_5x_3+cx_4y_5+c^2x_2y_5+y_7x_4+cx_2y_7+x_3y_7$$
$$-c^2y_5^2+y_6y_7)$$

$$y_4^{(n+1)} = \frac{1}{\sqrt{a}D}(-cy_6x_2 - cx_3y_8 - cx_3y_4 - cy_5y_6 + y_4^2 + y_8^2 + 2cy_6y_8 - cy_4y_7 - x_2y_4 - y_4x_4 - y_4y_5 - c^2x_3y_6 - c^2y_6y_7 + 2cy_4y_6 - cy_6x_4 - x_4y_8 - x_2y_8 - y_8y_9 - y_5y_8 + c^2y_6^2 + 2y_4y_8 - y_4y_9 - cy_6y_9 - cy_7y_8)$$

$$y_5^{(n+1)} = \frac{1}{\sqrt{a}D}(-y_5^2 - cy_6x_2 + y_5x_4 + x_4y_9 - x_4y_8 - x_2y_4 + y_4^2 - y_4x_4 - x_2y_8 - y_9^2 - c^2y_7^2 + c^2y_6^2 + y_8^2 + x_2y_5 - 2y_5y_9 - cy_6x_4 + c^2x_3y_7 - 2cy_7y_9 + 2cy_4y_6 - cx_3y_4 + cx_2y_7 - c^2x_3y_6 - cx_3y_8 + cx_4y_7 + cy_5x_3 + x_2y_9 + cy_9x_3 - 2cy_5y_7 + 2cy_6y_8 + 2y_4y_8)$$

$$y_6^{(n+1)} = \frac{1}{\sqrt{a}bD}(-2y_1 - cy_1y_3 + cy_1y_2 - cy_1x_1 + y_3^2 - y_2y_3 - 2cy_2 + 2cy_2y_3 - c^2x_1y_2 - cx_1y_2 - cx_1y_3 - c^2y_2y_3 + c^2y_2^2 - cy_2^2 - 2y_3 - cy_3^2 - x_1y_1 - y_2y_1 + y_3y_1 - x_1y_3)$$

$$y_7^{(n+1)} = \frac{1}{\sqrt{a}bD}(c^2x_1y_3 - 2cy_1y_3 + 2cy_1y_2 + y_3^2 - y_2^2 - 2cy_2 + 2cy_3 - c^2x_1y_2 + c^2y_2^2 - c^2y_3^2 + 2y_2 - 2y_3 - 2y_2y_1 + 2y_3y_1 - x_1y_3 + x_1y_2)$$

$$y_8^{(n+1)} = \frac{1}{\sqrt{a}bD}(-y_4y_5 - cy_6y_9 + 2cy_7y_9 - cy_7y_8 + y_5^2 + c^2y_9^2 + y_7^2 - cy_4y_9\ 2cy_5y_9 - x_3y_7 - x_2y_5 - y_7x_2 - y_7y_4 + 2y_7y_5 - c^2x_4y_9 - cx_4y_7 - cx_4y_5 - c^2y_8y_9 - cy_9x_3 - y_6y_7 - cy_5y_8 - y_6y_5 - cy_9x_2 - x_3y_5)$$

$$y_9^{(n+1)} = \frac{1}{\sqrt{a}bD}(y_7^2 + 2y_7y_5 - cy_9x_3 - cx_4y_5 + cy_6x_4 - x_3y_7 - x_2y_5 - 2cy_6y_8 - cy_9x_2 + x_2y_4 + x_3y_4 + y_6x_2 - 2y_6y_4 + c^2y_9^2 + 2cy_7y_9 + x_3y_6 - x_3y_5 + cx_3y_8 + cy_4x_4 - y_6^2 + c^2x_4y_8 + 2cy_5y_9 + cx_2y_8 - cx_4y_7 - 2cy_4y_8 - c^2x_4y_9 - y_4^2 - c^2y_8^2 + y_5^2 - y_7x_2$$

(8)

where $D = c^2 + 2cx_1 + c^2y_1^2 + x_1^2 + y_2^2 + 2y_2y_3 + y_3^2 + 2cy_1y_2 + 2cy_1y_3$. .

The local magnetization of the root x^0 has to be examined before we begin to analyze the phase diagram. Hence, the average magnetization $m^{(n)}$ for the nth generation is given by

$$m^{(n)} = -\frac{(A^2 - B^2)}{(A + 2B^2)}$$

where

$$A = 2 + 2y_3^2 + 2x_1^2 + 4x_1y_2 + 4x_1y_3 + 2y_2^2 + 4y_2y_3 + 4x_1 + 2x_4x_2 + 2x_4y_4 + 2x_4y_5 + 2y_8x_2 + 2y_8 + 2y_8y_5$$
$$+ 2y_9x_2 + 2y_9y_4 + 2y_9y_5 + 2x_3x_4 + 2x_3y_8 + 2x_3y_9 + 2y_6x_4 + 2y_6y_8 + 2y_6y_9 + 2y_7x_4 + 2y_7y_8 + 2y_7y_9$$
$$+ x_3^2 + 2x_3y_6 + 2x_3y_7 + y_6^2 + 2y_6y_7 + y_7^2 + 2y_1^2 + 2y_6x_2 + 2y_7x_2 + 2x_3x_2 + 2x_3y_4 + 2y_6y_4 + 4y_3y_1 + 2x_3y_5$$
$$+ 4x_1y_1 + 4y_2y_1 + 2y_7y_4 + 4y_1 + 4y_2 + x_4^2 + 2x_4y_8 + 4y_3 + 2x_4y_9 + y_8^2 + 2y_8y_9 + y_9^2 + x_2^2 + 2x_2y_4 + 2x_2y_5$$
$$+ y_4^2 + 2y_4y_5 + y_5^2 + 2y_7y_5 + 2y_6y_5.$$

and

$$B = 2 + 2y_3^2 + 2x_1^2 - 4x_1y_2 - 4x_1y_3 + 2y_2^2 + 4y_2y_3 + 4x_1 + 2x_4x_2 - 2x_4y_4 - 2x_4y_5 - 2y_8x_2 + 10y_8y_4 - 6y_8y_5$$
$$- 2y_9x_2 - 6y_9y_4 + 10y_9y_5 + 2x_3x_4 - 2x_3y_8 - 2x_3y_9 - 2y_6x_4 + 10y_6y_8 - 6y_6y_9 - 2y_7x_4 - 6y_7y_8 + 10y_7y_9 + x_3^2$$
$$- 2x_3y_6 - 2x_3y_7 + 5y_6^2 - 6y_6y_7 + 5y_7^2 + 2y_1^2 - 2y_6x_2 - 2y_7x_2 + 2x_3x_2 - 2x_3y_4 + 10y_6y_4 + 4y_3y_1 - 2x_3y_5 - 4x_1y_1$$
$$+ 4y_2y_1 - 6y_7y_4 - 4y_1 - 4y_2 + x_4^2 - 2x_4y_8 - 4y_3 - 2x_4y_9 + 5y_8^2 - 6y_8y_9 + 5y_9^2 + x_2^2 - 2x_2y_4 - 2x_2y_5 + 5y_4^2 - 6y_4y_5$$
$$+ 5y_5^2 + 10y_7y_5 - 6y_6y_5.$$

In the following section, we will apply some numerical simulation in order to investigate the behavior of the system of equations (8).

IV. MORPHOLOGY OF THE PHASE DIAGRAMS

An exact phase diagram can be numerically generated from the recurrence equation (8) in the $(K_BT/J_1, -J_2/J_3, J_3/J_1)$ space. This is done by letting $\alpha = K_BT/J_1$, $\gamma = -J_2/J_3$ and $\delta = J_3/J_1$ with $a = \exp(\alpha^{-1})$, $b = \exp(-\alpha^{-1}\gamma)$ and $c = \exp(\alpha^{-1}\delta)$. We then observe its behavior, starting from the following initial condition, which corresponds to the boundary condition $\sigma(W_{n+1}) \equiv 1$.

$$x_1^{(1)} = \frac{2ab^2c^2 + a^3 + a}{a^4b^3c^2 + a^2b}, \quad x_2^{(1)} = \frac{2a^2bc^2 + b^3 + b}{a^4b^3c^2 + a^2b},$$

$$x_3^{(1)} = \frac{2ac^2 + a^3b^2 + a}{a^4b^3c^2 + a^2b}, \quad x_4^{(1)} = \frac{2c^2 + b^2 + a^2}{a^4b^3c^2 + a^2b},$$

$$y_1^{(1)} = \frac{a^4b^3c^2 - a^2b}{a^4b^3c^2 + a^2b}, \quad y_2^{(1)} = \frac{ab^2c^2 - a^3}{a^4b^3c^2 + a^2b}, \quad y_3^{(1)} = \frac{ab^2c^2 - a}{a^4b^3c^2 + a^2b}, \tag{9}$$

$$y_4^{(1)} = \frac{a^2bc^2 - b^3}{a^4b^3c^2 + a^2b}, \quad y_5^{(1)} = \frac{a^2bc^2 - b}{a^4b^3c^2 + a^2b}, \quad y_6^{(1)} = \frac{ac^2 - a^3b^2}{a^4b^3c^2 + a^2b},$$

$$y_7^{(1)}=\frac{ac^2-a}{a^4b^3c^2+a^2b},\quad y_8^{(1)}=\frac{c^2-b^2}{a^4b^3c^2+a^2b},\quad y_9^{(1)}=\frac{c^2-a^2}{a^4b^3c^2+a^2b},$$

Consequently, if the system falls into the simplest of circumstances, it will exhibit the behavior of a fixed-point $(x_1^*, x_2^*, x_3^*, x_4^*, y_1^*, y_2^*, y_3^*, y_4^*, y_5^*, y_6^*, y_7^*, y_8^*)$. On the other hand, the point will correspond to the paramagnetic phase if $y_1^*, y_2^*, y_3^*, y_4^*, y_5^*, y_6^*, y_7^*, y_8^*, y_9^* = 0$. Whereas, in the case where $y_1^*, y_2^*, y_3^*, y_4^*, y_5^*, y_6^*, y_7^*, y_8^*, y_9^* \neq 0$, the point belongs to the ferromagnetic phase. Not only that, it is also possible for the system to be commensurate with a period p. The case $p = 4$ signifies an antiferromagnetic phase while $p = 4$ indicates an antiphase, which, for compactness purpose, is denoted by < 2 >.

Above all, the system may continue to be aperiodic. In this case, it can be strenuous to differentiate numerically whether a particular region is actually aperiodic, or simply having a remarkably high period. For this reason, the phase diagrams in this study only indicate periodic phases with period p for $p \leq 12$. We gather all the periodic phases with period $p > 12$, together with the aperiodic phase, into the modulated phase.

The resultant phase diagram on the plane (γ, α) with some fixed values of δ are shown in Figs 1 and 2. (Here: P - paramagnetic phase, F - ferromagnetic phase, AF - antiferromagnetic phase, PM – paramodulated phase, P3 - phase with period 3, , < 2 > - antiphase < + + - - >, < 3 > - antiphase < + + + - - - >, P5 - phase with period 5, P6 - phase with period 6, P7 - phase with period 7, P9 - phase with period 9, P11 - phase with period 11, and M - modulated phase).

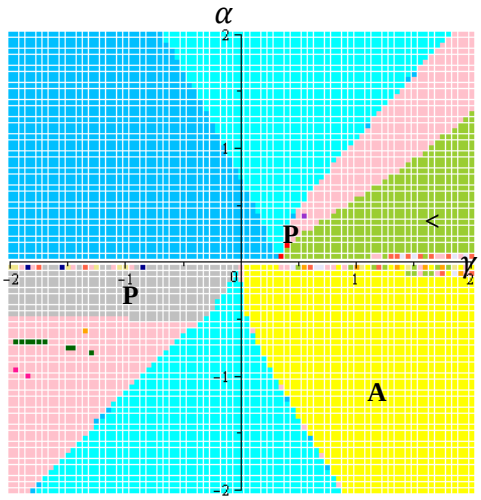

FIGURE 1. The phase diagram of α vs γ for δ = 0

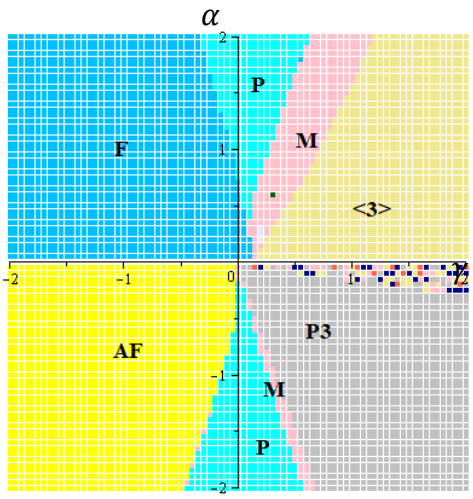

FIGURE 2. The phase diagram of α vs δ for γ = 0

For the phase diagram in Fig 1, we iterated the system for $\delta = 0$. We considered all possible signs of J_1 and J_2 and a plane that was divided into four quadrants was generated. As we can see, the first quadrant $(J_1 > 0, J_2 < 0)$ illustrates a paramagnetic, paramodulated, antiphase and modulated phase. On the other hand, a ferromagnetic and paramagnetic phase appear in the second quadrant $(J_1 > 0, J_2 > 0)$. Furthermore, the diagram consists of modulated and paramagnetic phase, a phase of period 3, as well as a tiny region of a period 7 phase in the third quadrant $(J_1 < 0, J_2 > 0)$.

Meanwhile, the fourth quadrant ($J_1 < 0, J_2 < 0$) consists of antiferromagnetic and paramagnetic phase.

In Fig 2, we have iterated the system for $\gamma = 0$. We can see that the first quadrant ($J_1 > 0, J_3 < 0$) consists of paramagnetic, modulated and antiphase < 3 >. The second quadrant ($J_1 > 0, J_3 > 0$) contains mainly ferromagnetic phase with a small region of paramagnetic phase. The third quadrant ($J_1 < 0, J_3 > 0$) shows of antiferromagnetic as well as a region of paramagnetic phase. Lastly, the fourth quadrant ($J_1 < 0, J_3 < 0$) comprises of phase of period 3, paramagnetic and modulated phase.

We have generated the phase diagrams for the model in (1) for the case $\delta \neq 0$ as we can see in Fig 3. The recurrence system of equations (8) was numerically iterated in order to produce the phase diagrams. We found that some additional phase diagrams exist when we included the binary interaction up to the third-nearest neighbour as compared to the case for $\delta = 0$. Hence, the third nearest-neighbour interaction carries a significant presence in the generation of the phase diagram for model (1).

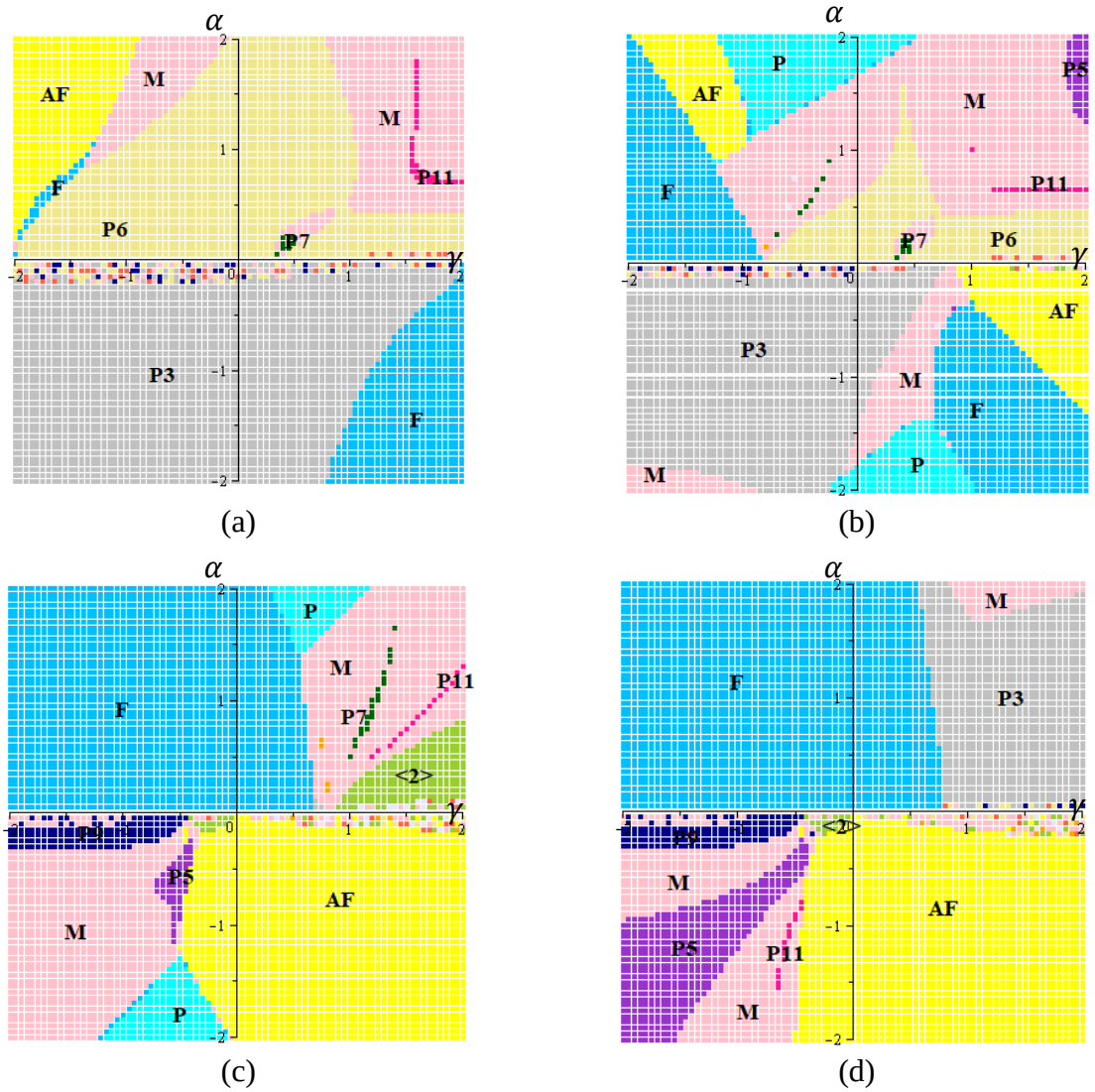

FIGURE 3. Phase diagram of α vs γ for the model with (a) δ = -1.25, (b) δ = -0.5, (c)) δ = 0.5 and (d)) δ = 1.25

Fig 3 illustrates the different phase diagrams according to their different δ values respectively. Fig 3(a) and 3(b) have been generated considering negative δ values. For δ = -1.25, there are antiferromagnetic, paramagnetic, phase of period 3, antiphase < 3 >, phase of period 11 as well as the modulated phases. Phase of period 3 dominated a large part of quadrants where the value of α are negative, alongside the ferromagnetic region. However, in Fig 3(b), there exist regions of paramagnetic, antiferromagnetic and modulated phases, which have not appeared in Fig 3(a).

We have seen before that when $\delta = 0$, there exists an antiphase region in the first quadrant. As the δ value gets more positive, the antiphase region gets smaller and eventually disappear as indicated by Fig 3(c) and 3(d). There is also the presence of the phase of period 5, which becomes larger as δ value becomes larger. Additional phases such as phase of period 7 and 11 are also present.

V. THE MODULATED PHASE

In this section, we will proceed to examine in detail the recurrence equation in (8). The advantage of this recurrence approach is that it allows us to show the existence of more commensurate phases with higher period than 12 in the set of modulated phases, albeit within very narrow region. This will be done by conducting an investigation on the wavevector with varying temperatures. We also will be looking into the Lyapunov exponent for the purpose of this study. Both of these methods are done in line with the methodology presented by Vannimenus [3]. For the numerical purpose, it is convenient to define the wavevector as

$$q = \lim_{N\to\infty} (n(N)/2N)$$

where $n(N)$ is the number of times the average magnetization changes sign during N successive iterations, as introduced by Vannimenus [3].

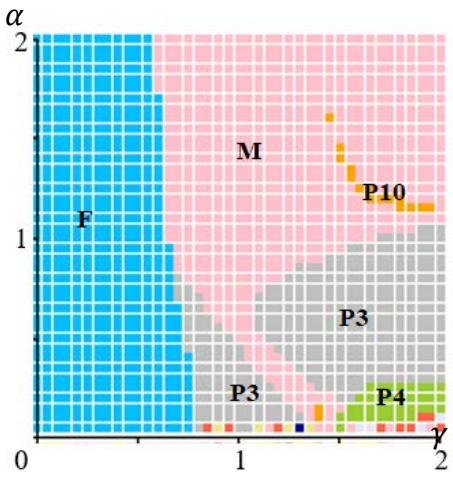

FIGURE 4. The phase diagram with $\delta = 0.75$, $0 \le \gamma \le 2$, $0 \le \alpha \le 2$.

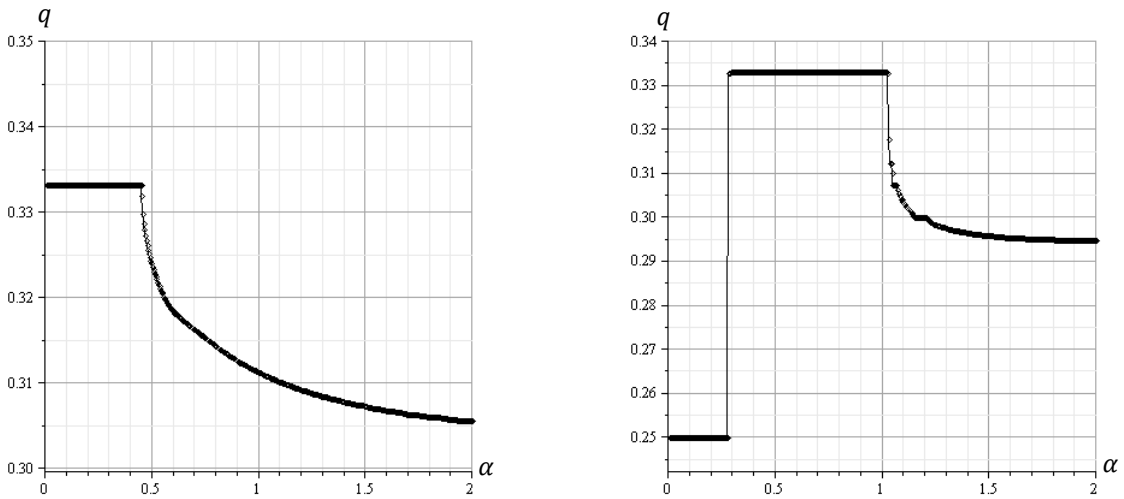

FIGURE 5. Variation of the wavevector q vs temperature for (a) $\delta = 0.75$, $\gamma = 1.00$ and (b) $\delta = 0.75$, $\gamma = 1.80$

Fig. 5 illustrates the variation of wavevector for $\delta = 0.75$ (refer the phase diagram in Fig 4) with different γ, which are $\gamma = 1.00$ and $\gamma = 1.80$. For Fig. 5(a), we can see that it starts with $q \approx 1/3$, which corresponds to the phase of period 3. Meanwhile, for Fig. 5(b), it starts with $q = 1/4$, which indicates the phase of period 4. These phases have excellent stability in terms of their periodicity, as it will give negative values when one computes for the Lyapunov exponents. These corresponding phases are accurately generated in the phase diagram in Fig 4.

The variation of wavevector with temperature showed us that the region of the modulated phase consists of different values of q. In determining that there is presence of phases with period higher than 12, we have to locate the locking steps in a particular wavevector graph. However, the interval for the locking steps might be exceptionally narrow. This leaves us with a more challenging task to distinguish whether a specific point behaves aperiodically or with an unusually high period.

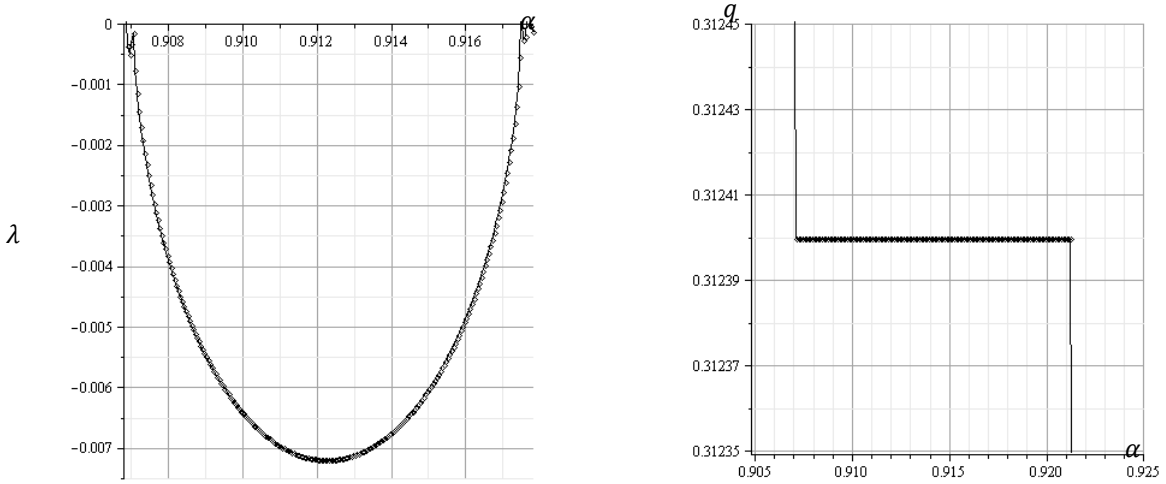

FIGURE 6. Variation of the Lyapunov exponent λ for $\delta = 0.75$, $\gamma = 1.00$ in the regions of commensurate steps $q \approx 5/16$ 6(b), enlarged from Fig 5(a).

Thus, Vannimenus [3] presented the solution of this problem by computing the Lyapunov exponent that is associated with the trajectory of the system. He asserted that the Lyapunov

exponents plays the role of general attractor the way that the logarithm of the largest eigenvalue plays for a simple fixed point. It convinces us whether an infinitesimal disturbance of the initial conditions will affect infinitesimally or give us a totally different trajectory.

The calculation of the Lyapunov exponent is carried out as follows. The recurrence equations in (8) are linearised around the successive points of the trajectory, yielding linear recurrence equations for the perturbations dx_1, dx_2, dx_3, dx_4, dx_5, dy_1, dy_2, dy_3, dy_4, dy_5, dy_6, dy_7, dy_8, dy_9), following Vannimenus [3]. In matrix, one has

$$V_{k+1} = \left(\delta' x_1, \delta' x_2, \delta' x_3, \delta' x_4, \delta' y_1, \delta' y_2, \delta' y_3, \delta' y_4, \delta' y_5, \delta' y_6, \delta' y_7, \delta' y_8, \delta' y_9\right)^T$$
$$= L_k\left(\delta x_1, \delta x_2, \delta x_3, \delta x_4, \delta y_1, \delta y_2, \delta y_4, \delta y_5, \delta y_6, \delta y_7, \delta y_8, \delta y_9\right)^T$$

where the matrix L_k depends on the iteration step. The Lyapunov exponent λ is obtained as

$$\lambda = \lim_{N\to\infty} (\log\|V_N\| / N)$$

where $\|V_N\|$ denotes the norm of the vector V. The existence of a stable limit cycle is only possible for negative exponents.

We fixed the value of $\gamma = 1.00$ and computed the corresponding Lyapunov exponent, which can be referred in Fig. 6(a). One stable region with $q \approx 5 / 16$ (Fig 6(b)) has been found, which indicates a limit cycle of period 16 in the interval $\alpha \in (0.9080, 0.9160)$. Referring to Fig. 7 and Fig 8, the value of $\delta = 0.75$, $\gamma = 1.80$ was chosen because q is closely approaching 11/36 and 15/49. These values have rather narrow intervals: which are from $\alpha \in (1.0750, 1.0770)$ (refer Fig. 7(b)) and $\alpha \in (1.0715, 1.0726)$ (refer Fig.8(b)), respectively.

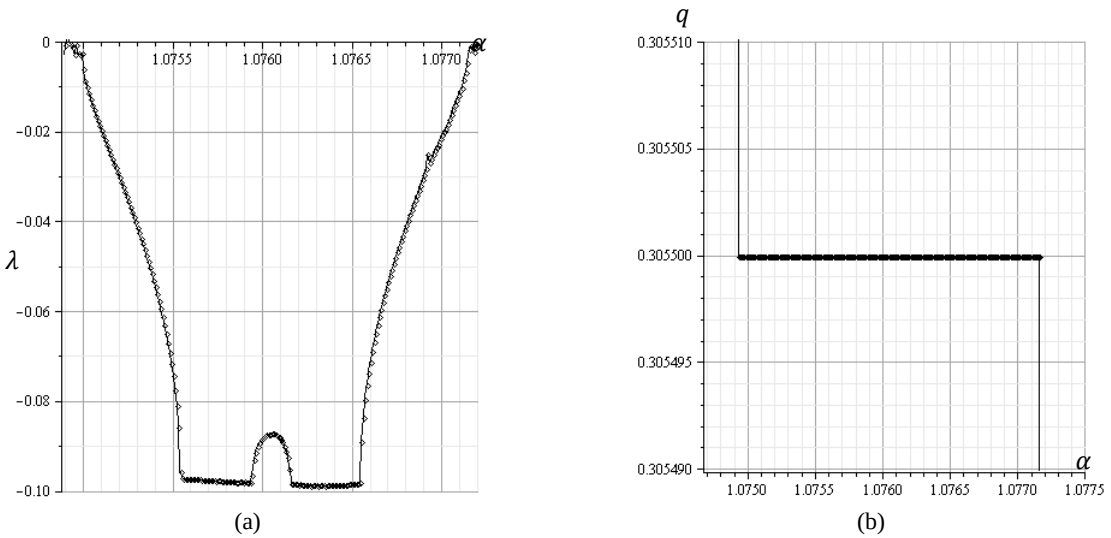

FIGURE 7. 7(a) Variation of the Lyapunov exponent λ for δ = 0.75, γ = 1.00 in the region of commensurate steps 7(b) $q \approx 11 / 36$, enlarged from Fig 5(b).

The stability of these phases in the modulated phase are investigated and presented in the calculation of the Lyapunov exponent (refer Fig. 7(a) and 8(a)). Fig. 7(a) shows the result for a cycle of period 36 with $N = 5000$. Not only that, a stability cycle for period 49 for $\delta = 0.75$, $\gamma = 1.80$ is presented (Fig. 8(a)). One can see that these phases are stable since they generated negative exponent in the computation of their Lyapunov exponents.

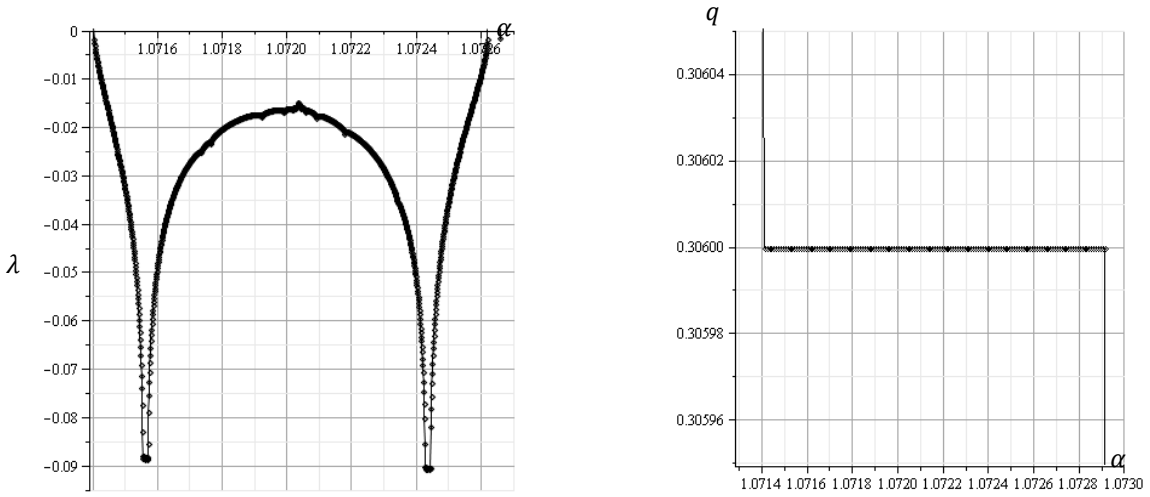

(a) (b)

FIGURE 8. 8(a) Variation of the Lyapunov exponent λ for δ = 0.75, γ = 1.00 in the region of commensurate steps 8(b) $q \approx 15 / 49$, enlarged from Fig 5(b).

VI. CONCLUSION

This paper focuses on the study of the phase diagrams of the Potts model on the Cayley tree with binary interactions up to the third nearest-neighbour. We have derived the recurrence system of equations, where the methodology in Vannimenus [3] is used in order to produce the system in (8). From the phase diagrams, we can see that the presence of the third nearest-neighbour interactions gives significant effect on the generation of the phase diagrams. The antiphase $< 2 >$ that exists when $\delta = 0$ eventually disappear as δ gets more positive. Furthermore, we have shown that there exist some commensurate phases with periods $p = 16$, 36 and 49 in the modulated phases. Finally, we investigated the variation of the wavevector with temperature in the modulated phase by using the Lyapunov exponent associated with the trajectory of the system. Therefore, we have shown that we can find the stability of a limit cycle of period $p > 12$ in the small region of the modulated phase.

For future investigation, we would suggest that the problem of the Potts model with competing interactions on the Cayley tree in the presence of external magnetic field is also considered in the study. A number of researchers has carried out the investigation using different approaches (Coutinho et al. [12], Mercado, Evertz and Gatringer [13], Akin and Temir [14]). Therefore, it would be interesting if we can study the phase transition in ferromagnetism as well as antiferromagnetism Potts system, using the recurrence approach.

ACKNOWLEDGMENTS

We would like to extend our gratitude to the reviewers, whose constructive comments and suggestions have helped to improve our manuscript. The work is supported by the International Islamic University Malaysia, under the research grant RIGS17-092-0667.

REFERENCES

1. R. Baxter, *Exactly Solved Models in Statistical Mechanics*, London: Academic Press, 1982, p. 2.
2. R. B. Potts, *Math. Proc. Cambridge.* **48**, 106-192 (1952).
3. J. Vannimenus, *Phys. Kondens. Mater.* **43**, 141-148 (1981).
4. S. Inawashiro, C. J. Thompson and G. Honda, *J. Stat. Phys.* **33**, 419-436, (1983).
5. A. M. Mariz, C. Tsallis and E. L. Albuquerque, *J. Stat. Phys.* **40**, 577-592, (1985).
6. N. Ganikhodjaev and M. H. Mohd Rodzhan, *J. Korean Phys. Soc* **66**, 1200-1206, (2015).
7. N. Ganikhodjaev, *Ph. Transit.* **89**, 1196-1202, (2016).
8. N. Ganikhodjaev and M. H. Mohd Rodzhan, *Malays. J. Math. Sci.* **10**, 167-180, (2016).
9. N. Ganikhodjaev, F. Mukhamedov and C. H. Pah, *Phys. Lett. A.* **373**, 33-38, (2008).
10. N. Ganikhodjaev, S. Temir and H. Akin, *J. Stat. Phys.* **137**, 701-715, (2009).
11. U. A. Rozikov, *Gibbs Measures on Cayley Trees*, Singapore: World Scientific Publishing, 1970.
12. S. Coutinho, W. Morgado, E. M. F. Curado, and L. da Silva, Phys. *Rev. B.* **74**, (2006).
13. Y. D. Mercado, H. G. Evertz, and C. Gattringer, *Comp. Phys. Comm.*, **183**, 1920-1927, (2012).
14. H. Akin and S. Temir, *Condens. Matter. Phys.*, **14**, 1-11, (2011).